

AD-A067 298

NAVAL RESEARCH LAB WASHINGTON D C

F/G 20/5

A HIGH-POWER, FREE-ELECTRON LASER BASED ON STIMULATED RAMAN BAC--ETC(U)

FEB 79 D B MCDERMOTT, T C MARSHALL

UNCLASSIFIED

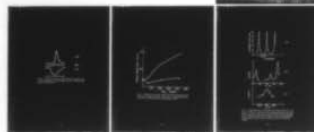
NRL-MR-3907

SBIE-AD-E000 283

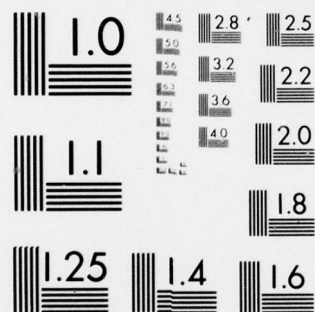
NL

| OF |

AD  
A067298



END  
DATE  
FILMED  
6 -79  
DDC



MICROCOPY RESOLUTION TEST CHART  
NATIONAL BUREAU OF STANDARDS-1963-A

P<sub>5</sub>

ADE 000 283

NRL Memorandum Report 3907

## A High-Power, Free-Electron Laser Based on Stimulated Raman Backscattering

D. B. McDERMOTT, T. C. MARSHALL, AND S. P. SCHLESINGER

*Plasma Laboratory, Columbia University,  
New York, New York 10027*

and

R. K. PARKER AND V. L. GRANATSTEIN

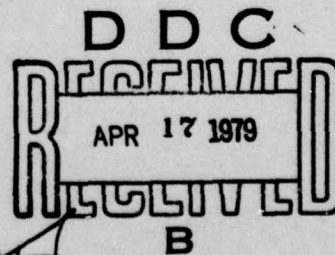
*Electron Beam Applications Branch  
Plasma Physics Division*

LEVEL III

AD A0 67298

DDC FILE COPY

February 16, 1979



NAVAL RESEARCH LABORATORY  
Washington, D.C.

Approved for public release; distribution unlimited.

79 03 09 014

SECURITY CLASSIFICATION OF THIS PAGE (When Data Entered)

REPORT DOCUMENTATION PAGE		READ INSTRUCTIONS BEFORE COMPLETING FORM
1. REPORT NUMBER NRL Memorandum Report 3907	2. GOVT ACCESSION NO.	3. RECIPIENT'S CATALOG NUMBER
4. TITLE (and Subtitle) A HIGH-POWER, FREE-ELECTRON LASER BASED ON STIMULATED RAMAN BACKSCATTERING		5. TYPE OF REPORT & PERIOD COVERED Interim report on a continuing NRL problem.
		6. PERFORMING ORG. REPORT NUMBER
7. AUTHOR(s) D. B. McDermott*, T. C. Marshall*, S. P. Schlesinger*, R. K. Parker and V.L. Granatstein		8. CONTRACT OR GRANT NUMBER(s)
9. PERFORMING ORGANIZATION NAME AND ADDRESS Naval Research Laboratory Washington, DC 20375		10. PROGRAM ELEMENT PROJECT, TASK AREA & WORK UNIT NUMBERS NRL Problem R08-59 Subtask RR0110941
11. CONTROLLING OFFICE NAME AND ADDRESS		12. REPORT DATE February 16, 1979
		13. NUMBER OF PAGES 14
14. MONITORING AGENCY NAME & ADDRESS (if different from Controlling Office)		15. SECURITY CLASS. (of this report) UNCLASSIFIED
		15a. DECLASSIFICATION/DOWNGRADING SCHEDULE
16. DISTRIBUTION STATEMENT (of this Report)  Approved for public release; distribution unlimited.		
17. DISTRIBUTION STATEMENT (of the abstract entered in Block 20, if different from Report)		
18. SUPPLEMENTARY NOTES *Plasma Laboratory, Columbia University, New York, New York 10027		
19. KEY WORDS (Continue on reverse side if necessary and identify by block number) Free electron laser                      Rippled magnetic field Stimulated Raman scattering Submillimeter wavelengths Intense relativistic electron beam		
20. ABSTRACT (Continue on reverse side if necessary and identify by block number) A free electron laser using an intense relativistic electron beam in a rippled magnetic field has been operated in the stimulated Raman scattering regime to yield megawatt-level radiation at submillimeter wavelengths; line-narrowing to $(\Delta\lambda/\lambda) \approx 2\%$ is reported. 4  <i>Delta lambda/lambda approximately</i>		

DD FORM 1473  
1 JAN 73

EDITION OF 1 NOV 65 IS OBSOLETE  
S/N 0102-014-6601

SECURITY CLASSIFICATION OF THIS PAGE (When Data Entered)

79 03 09 014

# A HIGH-POWER, FREE-ELECTRON LASER BASED ON STIMULATED RAMAN BACKSCATTERING

A tunable, submillimeter laser oscillator, based on a comparatively new principle independent of atomic transitions, is reported operating at megawatt power levels. The mechanism, referred to as stimulated Raman backscattering, involves the interaction of an intense relativistic electron beam (25 kA, 12 MeV) with a spatially rippled magnetic field<sup>1</sup> (period  $\ell_0 = 8$  mm). Unlike the "Ubitron,"<sup>2</sup> a non-relativistic device, the output radiation is Doppler-shifted to a wavelength much shorter than  $\ell_0$ . Furthermore, unlike the spontaneous radiation (Bremsstrahlung) from a low current relativistic beam in an "undulator,"<sup>3</sup> this device involves a three-wave parametric process<sup>4-7</sup> in which a scattered electromagnetic wave grows as a result of the interaction between a pump wave (here, a periodic magnetostatic ripple in the laboratory frame) and a negative-energy beam collective mode - in our case, the space charge wave. This three-wave process clearly distinguishes the present experiment from the free electron laser at Stanford University<sup>8</sup> which employed the tenuous beam in a linear accelerator. That experiment, involving no collective modes, was operated in the Compton regime; the gain was low (i.e.  $\Gamma_L L \ll 1$  where  $\Gamma_L$  is the amplitude growth rate and  $L$  is the length of the interaction region) and salient laser parameters

Note: Manuscript submitted November 13, 1978.

BY		<input checked="" type="checkbox"/> Section <input type="checkbox"/> Action <input type="checkbox"/>
DISTRIBUTION/AVAILABILITY CODES		
Dist.	and/or	SPECIAL
A		



such as gain<sup>5</sup> and saturated power level<sup>9</sup> were a strong function of  $L$ . In contrast, the present experiment is in the high-gain regime  $\Gamma_L L > 1$  where  $\Gamma_L$ <sup>4-6</sup> and saturated efficiency<sup>5</sup> depend only on the intrinsic properties of the electron beam and the ripple amplitude, but not on finite system length.

The properties of the interaction, a convective<sup>1</sup> beam instability, were first studied<sup>10-12</sup> in the superradiant mode, where the beam amplifies noise radiation in a single-pass system. Spectral studies<sup>12</sup> of the emission show that the scattered frequency appropriate to our circumstance is

$$\omega_s = \frac{2\pi v / \ell_0 - \omega_p / \gamma}{1 - \beta}$$

where  $\gamma = (1 - \beta^2)^{-\frac{1}{2}}$ ,  $\beta = v/c$ ,  $v$  is the electron speed along the magnetic axis and  $\omega_p = (4\pi n e^2 / \gamma m_0)^{\frac{1}{2}}$ ; the density ( $n$ ) is measured in the lab frame. The linewidth of the superradiant emission,<sup>12</sup> which is greater than 10%, is attributable partly to beam-energy spread and partly to the dispersive growth rate.<sup>13</sup>

Feedback of the output signal using a quasi-optical cavity with two mirrors should improve<sup>1</sup> the performance, providing that a) excitation of other unstable modes does not occur, that b) the accelerator pulse length permits several bounces of the radiation in the optical resonator, and that c) the accelerating voltage remains constant during that interval. The first requirement is met because scattering from the cyclotron idler mode is damped<sup>14</sup> due to the high beam densities in our experiment. The accelerator we have used (NRL's VEBA<sup>15</sup>) only marginally fits the last two requirements: the

pulse remains strong for about 40 nsec, permitting approximately four passes of radiation, and the voltage unfortunately has a 20 nsec periodic ripple which ranges between 5-10% of peak energy. Since  $\lambda_s \approx l_0/2\gamma^2$  one expects the scattered radiation to spread over a wavelength range:

$$\Delta\lambda_s/\lambda_s \approx 2 \Delta\gamma/\gamma \approx 10-20\%$$

Nevertheless, the coherence of the laser signal is found to be better by nearly an order of magnitude. Obviously, better results can be expected from an accelerator specially suited to our requirements.

The experimental configuration is shown in Fig. 1; the cylindrical shell electron beam (dia. = 4.5 cm; thickness - 1 mm), field emitted from a graphite cathode, is adiabatically expanded through the 2" O.D. drift tube using magnetic field profiling, thereby locating the electrons within the ray path of a set of plane, polished, adjustable aluminum mirrors separated by 150 cm. The mirrors, with O.D. = 5 cm and I.D. = 1.8 cm, permit about 2% of the intercavity power to be diffraction-coupled into a lightpipe. The cathode end of the cavity was unavoidably lossy. The mirrors must be carefully aligned to within  $.05^\circ$  with the aid of an optical laser beam so that the reflected radiation returns through the amplifying medium.

The 40 cm "undulator" is constructed of insulated aluminum rings through which current flows in alternating directions<sup>16</sup> with an 8 mm period. The undulator produces a magnetostatic ripple field having a radial amplitude ( $B_1$ ) up to 400 G at the radius of the electron beam.

Figure 2 shows the output signal with the mirrors aligned (2a) and misaligned (2b), together with the accelerator voltage (2c). The laser signal (2a) is not only much stronger than the superradiant signal (2b) but it is also more regular; it frequently shows a step-structure with output increasing after a 10 nsec interval which is the cavity bounce time for the radiation. During the tail of the voltage pulse, when the beam  $\gamma$  has dropped appreciably, the emitted power quickly decreases implying absorption of cavity power (negative gain) by off-resonance electrons. (Amplification by the electron beam depends on the difference between the wavelength of the radiation it would superradiantly emit and the wavelength of the existing cavity radiation. An analysis using single-electron dynamics<sup>17</sup> shows the laser gain depends on the detuning.) After the electron beam shuts off, the power exponentially declines due to leakage of radiation from the cavity; we determine the cavity  $Q \approx 3$  from the exponentiation rate. The output power is 0.1-1.0 MW, implying an intercavity power level of  $\approx 10$  MW.

Figure 3 shows the dependence of the power on ripple amplitude for both the superradiant and lasing mode of operation; the output increases rapidly for the laser as the pump is increased above  $\approx 80$  G amplitude. Earlier experiments<sup>12,16</sup> under superradiant conditions (travelling-wave amplification) showed that the scattered power is exponential in field ripple amplitude; the superradiant power in this experiment (lower curve, Fig. 3) is obviously quite small.



The dependence of the laser output upon the pump as observed here (upper curve, Fig. 3) is more nearly characteristic of conventional laser performance.<sup>18</sup>

Measurement of wavelength and spectral width ( $\Delta\lambda_s/\lambda_s$ ) were made with a quasi-optical version<sup>11</sup> of a Fabry-Perot interferometer. Two plane, parallel screen meshes were mounted in the light pipe; the adjustable gap ( $d$ ) between the reflectors is measured with a micrometer. A crystal detector monitors the incoming power and another crystal detects the signal transmitted through the Fabry-Perot; thereby, shot-to-shot power fluctuations are normalized out. The distance between maxima yields  $\lambda_s/2$  and the normalized width of a maximum yields the spectral width ( $\Delta\lambda_s/\lambda_s = \Delta d/d$ ) or instrumental resolution,<sup>19</sup> whichever is greater. The resolution is influenced by mesh reflectivity ( $\approx 40\%$ ) and parallelism, which contribute to a limiting resolving power  $\approx 50$ . Shots where the accelerator voltage was not reproducible were discarded, to remove variations in  $\lambda_s$  caused by variations of  $\gamma$ .

Figure 4a shows the performance of a Fabry-Perot, of similar construction to the one used for these laser measurements, using coherent power from a 3 mm Klystron. The instrumental width of the maxima, or the fringe "contrast", is due to a mirror reflectivity  $\approx 70\%$  in this example. In Fig. 4b we show data for the Fabry-Perot pattern of the laser output at the same time in voltage history for each shot, from which we conclude  $\lambda_s = 400\mu$ . This wavelength is in

agreement with that given by eq. (1) using  $\gamma = 3.4$  and  $\omega_p/2\pi = 8$  GHz (obtained from the diode voltage, beam current, and witness plate measurements). The variation in amplitude of the maxima in Fig. 4b is caused by slightly missing the optimum resonance location as the resonator gap is narrowed mechanically. The radiation from stimulated backscattering off the cyclotron mode, which should occur at  $\lambda_s \approx 500\mu$  is not found in this system.

In Fig. 4c we show in detail a maximum located at  $m - 2d/\lambda \approx 20$ ; it is clear  $\Delta\lambda_s/\lambda_s \approx 2\%$ , which is essentially the limit of instrumental resolution. All measurements shown in Fig. 4b,c were taken during peak power; the Fabry-Perot pattern was also clearly observed at an earlier instant when the laser power was half as large; in that case  $\Delta\lambda_s/\lambda_s \approx 4\%$ .

When the laser mirrors were removed, a measurement of the spectral linewidth under conditions corresponding to the lower curve in Fig. 3 gave  $\Delta\lambda_s/\lambda_s \approx 10\%$ . This result is in agreement with previous measurements of spectral width in this mode of operation.<sup>12</sup> Thus, a considerable improvement in coherence is effected by the addition of regenerative feedback in the laser cavity, and the linewidth narrows as power increases, in accord with conventional laser performance.<sup>20</sup>

In the superradiant mode of operation (no mirrors, single-pass gain) it has been found that increasing power output can be obtained by increasing the pump amplitude; however, this increases  $\Delta\lambda_s/\lambda_s$ .<sup>12,13</sup> The laser cavity configuration provides a signal of improved coherence as the power increases.

Finally, the present experiment may be compared with theoretical analyses. The expression for gain in the stimulated Raman regime is<sup>4,6</sup>

$$\Gamma L = [(e\beta_{\perp}/m_0)^2 \omega_p L^2 \epsilon_0 / 4\pi\gamma c^3]^{\frac{1}{2}} \quad (2)$$

For the parameters of the present experiment Eq. (2) yields  $\Gamma L = 1.6$ ; thus, it is quite plausible that several passes of radiation through the cavity are necessary and sufficient to pass the lasing threshold. The theoretical expression for saturated efficiency is<sup>5,21</sup>

$$\eta = \omega_p \epsilon_0 / 4\pi(\gamma-1)c \quad (3)$$

which is calculated as 4%. The measured 1 megawatt output corresponds to 0.003% efficiency. Thus, as might be expected with the limited 40 nsec time duration of the electron beam, or as might be deduced from Fig. 3, the wave amplification process is far from saturation.

Research supported by AFOSR (Grant F44620-75-C-0055) and ONR.

# REFERENCES

1. D. B. McDermott, T. C. Marshall, S. P. Schlesinger, Comments Plasma Phys. Cont. Fusion 3 165 (1978).
2. R. M. Phillips, IRE Trans. Elect. Devices ED-7, 231 (1960).
3. H. Motz, J. Appl. Phys. 22, 527 (1951).
4. P. Sprangle, V. L. Granatstein and L. Baker, Phys. Rev. A 12, 1697 (1975).
5. J. T. Kwan, J. M. Dawson and A. T. Lin, Phys. Fluids 20, 581 (1977).
6. N. M. Kroll and W. A. McMullin, Phys. Rev. A 17, 300 (1978).
7. V. L. Granatstein, S. P. Schlesinger, M. Herndon, R. K. Parker and J. A. Pasour, Appl. Phys. Lett. 30, 384 (1977).
8. D. A. G. Deacon, L. R. Elias, J. M. J. Madey, G. J. Ramian, H. A. Schwettman, and T. I. Smith, Phys. Rev. Lett. 38, 892 (1977).
9. F. A. Hopf, P. Meystre, M. O. Scully, and W. H. Louisell, Phys. Rev. Lett. 37, 1342 (1976).
10. P. E. Efthimion and S. P. Schlesinger, Phys. Rev. A 15, 633 (1977).
11. T. C. Marshall, S. Talmadge, and P. Efthimion, Appl. Phys. Lett. 31, 320 (1977).
12. R. M. Gilgenbach, T. C. Marshall, S. P. Schlesinger, "Spectral Properties of Stimulated Raman Radiation from an Intense Relativistic Electron Beam," submitted to Phys. Fluids.
13. T. J. T. Kwan, thesis, UCLA Physics Dept. report PFG-354 (May 1978), p. 117.
14. R. M. Gilgenbach, T. C. Marshall, and S. P. Schlesinger, "Cyclotron Harmonic Damping in Raman Scattering from an Intense Relativistic Electron Beam," submitted to Phys. Fluids.
15. R. K. Parker and M. Ury, IEEE Trans. NS-22, 983 (1975).
16. T. C. Marshall, R. M. Gilgenbach, F. Sandel, in Proc. of the 2nd International Topical Conf. on High Power Electron and Ion Beam Research and Technology, 1977, edited by J. A. Nation and R. N. Sudan (Cornell University, Ithaca, N.Y.), p. 697.



17. W. B. Colson, Phys. of Quantum Electronics, 5.
18. A. Yariv, "Introduction to Optical Electronics," p. 101, Holt, Rinehart and Winston (1971).
19. M. Born and E. Wolf, "Principles of Optics," p. 327, Pergamon Press (1959).
20. Reference 17, p. 265.
21. P. Sprangle and A. T. Drobot, J. Applied Phys. (to be published).

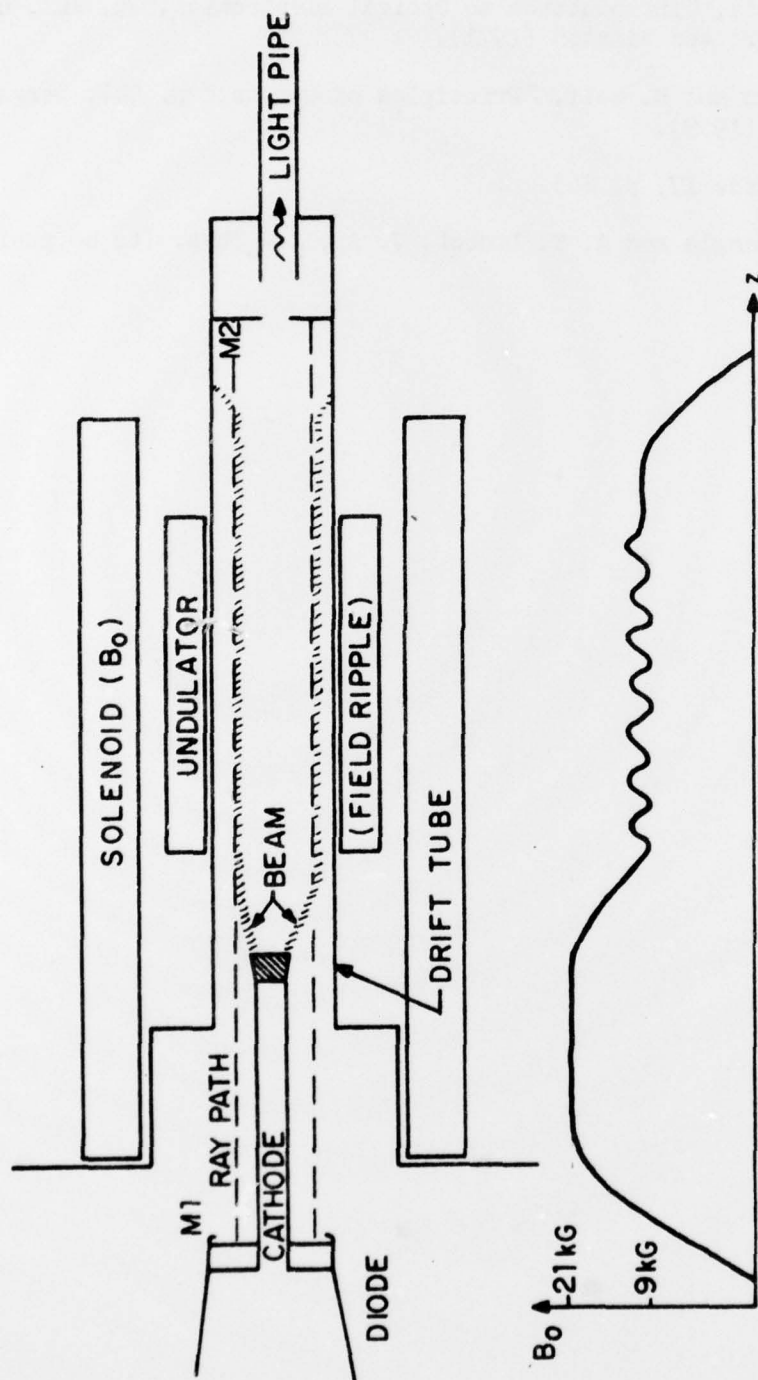


Fig. 1 — The Apparatus is attached to the NRL VEBA accelerator. The beam emerges from a 2.8 cm dia. cathode and the operating pressure is  $\lesssim 10^{-4}$  torr in the diode. Radiation is emitted into the light pipe through a polyethylene window which forms the vacuum seal.

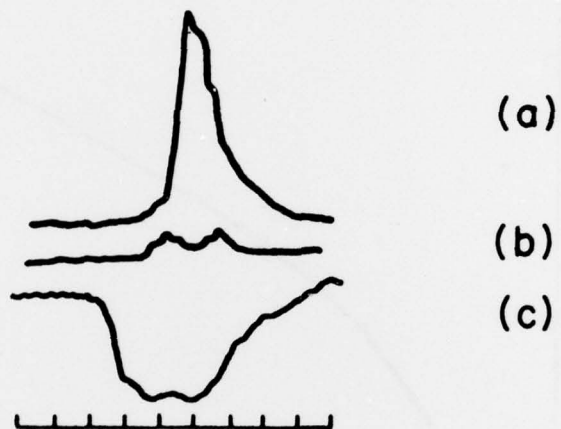


Fig. 2 — (a) The laser signal; (b) signal from the apparatus with a mirror misaligned; (c) diode voltage, 1.25 MV. The horizontal axis is time, 20 nsec/div.

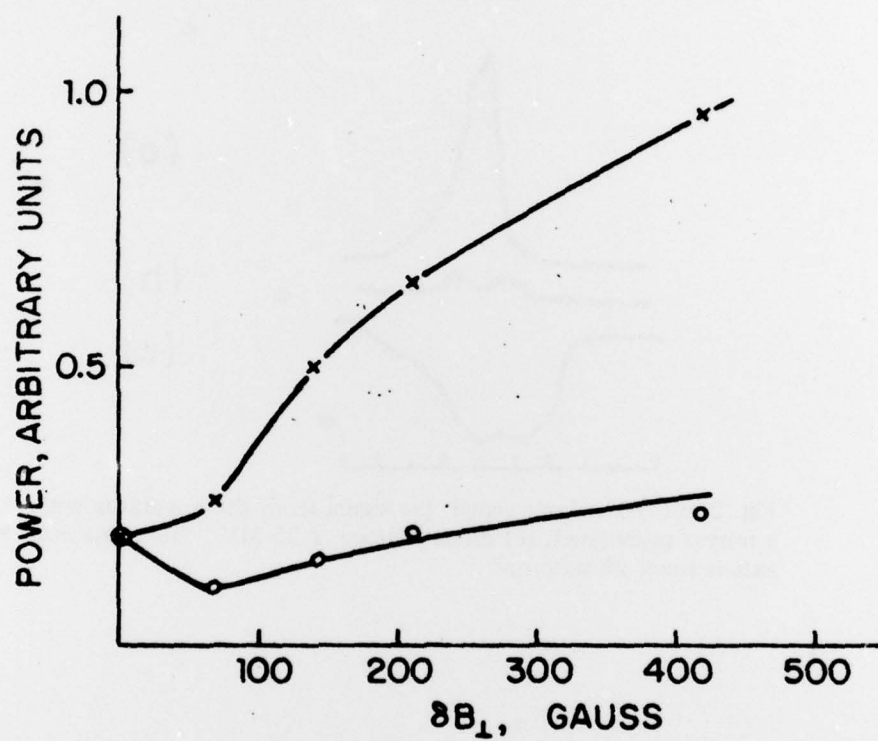


Fig. 3 — Dependence of power output upon pump amplitude (radial component of ripple field  $S\beta_{\perp}$ ). Upper curve: (x) system lasing; (O) lower curve, anode mirror removed (superradiant mode).



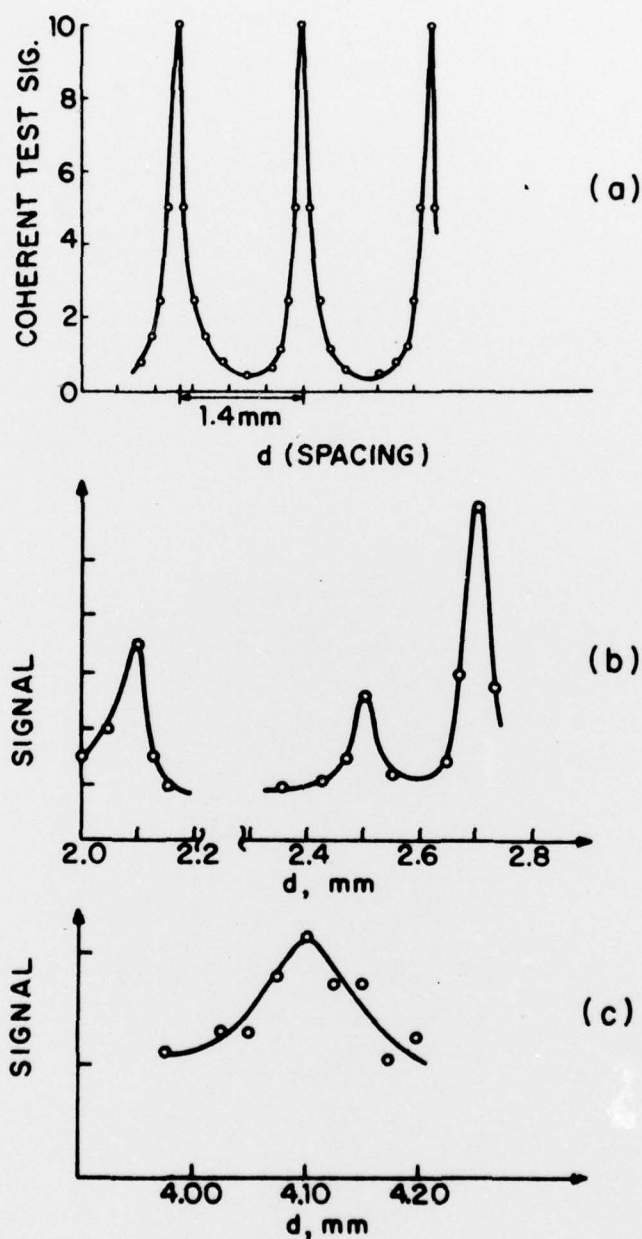


Fig. 4 — Fabry-Perot data. (a) Response to a coherent wave at  $\lambda = 2.8$  mm,  $d \approx 5\lambda/2$ ; (b), (c) show the laser signal analyzed by the Fabry-Perot; (b) shows a wide scan and (c) detail under optimum resolving power  $\approx 50$ . The break in the abscissa in (b) is due to readjustment of the apparatus which caused a stepwise motion of Fabry-Perot carriage.